HHS Public Access

Author manuscript

Cancer Lett. Author manuscript; available in PMC 2022 May 09.

Published in final edited form as:

Cancer Lett. 2020 November 28; 493: 143–155. doi:10.1016/j.canlet.2020.08.015.

Integrin α4 up-regulation activates the hedgehog pathway to promote arsenic and benzo[α]pyrene co-exposure-induced cancer stem cell-like property and tumorigenesis

Jie Xie[a,b], **Ping Yang**[a,c], **Hsuan-Pei Lin**[a], **Yunfei Li**[a], **Marco Clementino**[a], **William Fenske**[a], **Chengfeng Yang**[a], **Chunhong Wang**[b], **Zhishan Wang**[a,*]

[a]Department of Toxicology and Cancer Biology, University of Kentucky College of Medicine, Lexington, KY, USA

[b]School of Health Sciences, Wuhan University, Wuhan, Hubei, P.R. China

[c]School of Public Health, Guangzhou Medical University, Guangzhou, Guangdong, P.R. China

Abstract

Arsenic and benzo[α]pyrene (BaP) are widespread carcinogens and important etiology factors for lung cancer. Moreover, arsenic and BaP co-exposure displays a significantly stronger effect in inducing lung cancer than arsenic or BaP exposure alone. This study was performed to investigate the basic mechanism of the synergistic carcinogenic effect of arsenic and BaP co-exposure. It was found that integrin α4 (ITGA4) expression levels are significantly up-regulated and the Hedgehog pathway is highly activated in arsenic plus BaP co-exposure-transformed human bronchial epithelial cells. Either ITGA4 downregulation or Hedgehog pathway inhibition in the co-exposure-transformed cells significantly reduced their cancer stem cell (CSC)-like property and tumorigenicity. It was determined that ITGA4 downregulation leads to the inhibition of the Hedgehog pathway activation, which is achieved by increasing suppressor of fused (SUFU) protein stability through reducing the PI3K/Akt signaling. Moreover, stably overexpressing SUFU in the co-exposure-transformed cells significantly reduces their CSC-like property and tumorigenicity. These findings indicate that ITGA4 up-regulation activates the Hedgehog pathway to enhance the CSC-like property and tumorigenicity of arsenic and BaP co-exposure-transformed cells, offering new mechanistic insight for the synergistic carcinogenic effect of arsenic and BaP co-exposure.

*Corresponding author. Department of Toxicology and Cancer Biology, University of Kentucky College of Medicine, 254 HSRB, 1095 Veterans Drive, Lexington, KY, USA. Zhishan.wang@uky.edu (Z. Wang).

Author contributions

Jie Xie: Conceptualization; Methodology; Data curation; Formal analysis, Writing - original draft. **Ping Yang, Hsuan-Pei Lin, Yunfei Li, Marco Clementino:** Data curation; Methodology; Validation. **William Fenske:** Writing - review & editing. **Chengfeng Yang:** Conceptualization; Methodology; Writing - review & editing. **Chunhong Wang:** Supervision; Writing - review & editing. **Zhishan Wang:** Conceptualization; Project administration; Supervision; Funding acquisition; Methodology; Writing - review & editing.

Declaration of competing interest

The authors declare that they have no conflicts of interests.

Appendix A. Supplementary data

Supplementary data related to this article can be found at https://doi.org/10.1016/j.canlet.2020.08.015.

Keywords

Arsenic and benzo[α]pyrene co-exposure; ITGA4; GLI-1; Hedgehog pathway; CSC-Like property

1. Introduction

Humans are often exposed to mixtures of environmental pollutants. Studies have shown that the toxic effects of the mixture exposures could be significantly different from the sum of the effects of exposures to individual pollutants [1,2]. However, our understanding on the mechanisms of the adverse health effects of environmental mixture exposures is limited [3,4]. Understanding the mechanism of toxic effects of environmental mixture exposures may identify molecular targets to prevent and treat human diseases resulting from mixture exposures.

Arsenic and benzo[α]pyrene (BaP) are among the most common environmental carcinogens causing lung cancer in humans. While occupational arsenic exposure occurs mainly via inhalation of arsenic vapor-contaminated air, general population arsenic exposure mainly results from oral ingestion by consumption of arsenic-contaminated drinking water or food [5]. BaP is usually produced when organic matters are not completely burned and high concentrations of BaP are found in cigarette smoke and well-done barbecue meat. General population BaP exposure could happen either via inhalation of cigarette smoke or from oral ingestion by consumption of BaP-contaminated food. Given the fact that millions of people are consuming arsenic-contaminated water, and that cigarette smoking and meat barbecuing are common behaviors in many regions, human co-exposure to arsenic and BaP could be common, representing a significant environmental health issue. Early studies showed that arsenic and BaP co-exposure via intratracheal instillation significantly increases lung cancer risk in rats and hamsters [6,7]. Moreover, our recent study revealed that arsenic exposure via drinking water in conjunction with BaP exposure via oral gavage significantly increases lung tumorigenesis in mice [8]. These findings demonstrate that arsenic and BaP co-exposure causes a more potent lung tumorigenic effect than arsenic or BaP exposure alone. However, the mechanism of the synergistic lung tumorigenic effect of arsenic and Bap co-exposure has not been well understood.

Integrin α4 (ITGA4) is a member of the integrin family of heterodimeric transmembrane proteins, which play important roles in cell survival, proliferation, migration, invasion, and tumor growth and metastasis [9]. ITGA4 is one of the least studied integrins in the family [10]. Up-regulation of ITGA4 expression has been reported in several types of cancer, playing important roles in tumor cell invasion and tumor metastasis [11]. However, little is known about the role of ITGA4 in tumor development. The Hedgehog pathway is a highly conserved developmental signaling pathway, playing critical roles in many physiological processes during embryonic development [12,13]. The key components of the Hedgehog pathway include Hedgehog ligands, the transmembrane receptors Patched (Ptch) and Smoothened (SMO), the transcription factors glioma-associated oncogene homologs (GLI) and the central negative regulator of the pathway Suppressor of Fused (SUFU) that sequesters GLI transcription factors in an inactive complex [14,15]. The canonical

Hedgehog pathway activation is initiated by the binding of Hedgehog ligands to Ptch, which frees SMO, leading to the activation of GLI transcription factors [16,17]. Abnormal activation of the Hedgehog pathway during the adult stage has been shown to play crucial roles in tumorigenesis [12,13]. However, how the Hedgehog pathway is activated during the tumorigenic process is not well known.

Our recent study using cell culture and mouse models demonstrated that arsenic and BaP co-exposure acts synergistically in inducing cell malignant transformation, cancer stem cell (CSC)-like property and lung tumorigenesis [8]. This study was performed to further investigate the underlying mechanism. It was found that arsenic and BaP co-exposure greatly up-regulates the expression of ITGA4, activating the phosphoinositide 3-kinase (PI3K)/Akt pathway. Increased Akt activity reduces SUFU protein stability and levels, leading to activation of the Hedgehog pathway and enhancing arsenic and BaP co-exposure-induced cancer stem cell (CSC)-like property and tumorigenesis. This study provides the first evidence showing that ITGA4 signaling activates the Hedgehog pathway in tumor cells. Moreover, the findings from this study not only offer new mechanistic insight for the synergistic tumorigenic effect of arsenic and BaP co-exposure, but also provide evidence for targeting ITGA4 and the Hedgehog pathway to prevent and treat lung tumors resulting from arsenic and BaP co-exposure.

2. Materials and methods

2.1. Cell culture

Immortalized non-tumorigenic human bronchial epithelial BEAS-2B cells were obtained from American Type Culture Collection (ATCC, Manassas, VA). The passage-matched Control BEAS-2B cells (BEAS-2B-Control), chronic low dose of arsenic ($NaAsO_2$, 1 μM, Sigma) (BEAS-2B–As), or BaP (2.5 μM, Sigma) (BEAS-2B–BaP) exposure alone and co-exposure-transformed BEAS-2B cells (BEAS-2B–As + BaP) were generated, characterized and reported in our recent study [8]. Briefly, BEAS-2B cells were continuously exposed to a vehicle control, arsenic ($NaAsO_2$, 1 μM) or BaP (2.5 μM) alone, or arsenic plus BaP (1 μM of $NaAsO_2$ + 2.5 μM of BaP) for 30 weeks. Arsenic and BaP exposure-induced cell transformation, CSC-like property and tumorigenesis were determined by the soft agar colony formation assay, suspension culture sphere formation assay and nude mouse tumorigenesis assay, respectively [8]. All BEAS-2B cells were cultured in Dulbecco's Modified Eagle Medium (DMEM, Invitrogen) supplemented with 5% fetal bovine serum (FBS, Sigma), 1% penicillin/streptomycin (10,000 U/mL, Gibico).

2.2. Microarray analysis

Total RNA samples were isolated from the passage-matched BEAS-2B-Control, BEAS-2B–As, BEAS-2B–BaP, and BEAS-2B–As + BaP cells using the TRIzol reagent (Invitrogen, Carlsbad, CA) according to the manufacturer's protocol. The RNA samples in triplicate were submitted to Arraystar Inc. (Rockville, MD) for microarray analysis. Microarray data analysis was done by Arraystar Inc. The microarray raw data was deposited to the National Center for Biotechnology Information (NCBI)'s data repository (Access ID: GSE149605).

2.3. Generation of ITGA4 stable knockdown and SUFU stable overexpression cells

The arsenic and BaP co-exposure-transformed cells (BEAS-2B–As + BaP) were used for lentiviral particle transduction to generate ITGA4 stable knockdown or SUFU stable overexpression cells. Non-targeting control short hairpin RNA (shRNA) lentiviral particles (pZIP-hCMV-ZsGreen-Puro-Control shRNA), ITGA4-specific targeting shRNA lentiviral particles (pZIP-hCMV-ZsGreen-Puro-ITGA4 shRNA), overexpression vector control lentiviral particles (pTOL-hCMV-Puro), and SUFU overexpression lentiviral particles (pTOL-hCMV-Puro-SUFU) were obtained from Transomic Technologies (Huntsville, AL). Forty-eight hours (h) after the lentiviral particle transduction, BEAS-2B–As + BaP cells were selected with puromycin (1 μg/mL) following the procedures described in our recent studies [18]. The ITGA4 stable knockdown or SUFU stable overexpression efficiency in BEAS-2B–As + BaP cells were confirmed by Western blot analysis.

2.4. Soft agar colony formation assay

The soft agar colony formation assay was performed following our previously published protocol [19]. Briefly, Normal melting point agar (4 mL of 0.6% agar in DMEM) was placed in each 60-mm cell culture dish as the bottom layer of agar and allowed to solidify for 1 h at room temperature. BEAS-2B–As + BaP-control shRNA cells and ITGA4 stable knockdown (BEAS-2B–As + BaP-ITGA4 shRNA) cells were collected, counted, suspended in DMEM and mixed with the lower melting point agar. The cell-agar mixture containing 2 mL of cell suspensions (0.5×10^4 cells/mL) and 2 mL of lower melting point agar (0.8% agar in DMEM) was placed above the bottom agar. Two mL of DMEM containing 10% FBS was added to the top agar after it was solidified. Dishes were incubated at 37 °C in a humidified atmosphere containing 5% CO_2. After a 4-week incubation, soft agar colonies were stained with 0.002% crystal violet, photographed and counted (if > 100 μm). The results are presented as mean ± standard deviation (SD).

2.5. Serum-free suspension culture sphere formation assay

The sphere formation assay was conducted as previously described [20,21]. Briefly, cells were collected by trypsinization, well-suspended in serum-free DMEM supplemented with 1 × B27 (Invitrogen, Carlsbad, CA), human recombinant epidermal growth factor (20 ng/mL. R&D, Minneapolis, MN), basic fibroblast growth factor (20 ng/mL, R&D Systems, Minneapolis), and heparin (4 μg/mL, Sigma), and cultured in ultralow attachment 24-well plates for 10 days (Corning, Corning, NY). Two thousand five hundreds cells were seeded in each well. At the end of the 10-day culture, spheres with diameters > 100 μm were counted and photographed under an inverted microscope. The results are presented as mean ± standard deviation (SD).

2.6. Western blot analysis

Cultured cells were collected by trypsinization, pelleted, washed with PBS and lysed with cell lysis buffer following our published protocol [22,23]. The bicinchoninic acid (Bio-rad) reaction was performed to quantify cellular protein concentrations. Equal amounts of protein samples (20–30 μg) were separated by sodium dodecyl sulfate-polyacrylamide gel electrophoresis (SDS-PAGE) and transferred to 0.45 μm of polyvinylidene fluoride

membranes (PVDF, Millipore, Billerica MA, USA). The membranes were blocked with 5% milk in PBS Tween 20 (PBST) buffer for 1 h at room temperature and then incubated with the following primary antibodies: anti-ITGA4 (1:1000), anti-GLI-1 (1:500), anti-SUFU (1:1000), anti-SMO (1:1000), anti-SHH (1:1000), anti-Ptch-1 (1:500), anti-p-Akt (1:1000), anti-Akt (1:1000), anti-p-ERK (1:1000), anti-ERK (1:1000) or β-actin (1:8000) overnight at 4 °C. After overnight incubation, the membranes were washed with PBST and incubated with HRP-conjugated secondary antibody (goat anti-rabbit IgG 1:2000 or goat anti-mouse IgG 1:5000) for 1 h at room temperature. Immuno-signals were visualized using the Amersham Imager 680 (GE Healthcare Life Sciences, Marlborough, MA, USA). The intensities of protein bands were quantified by the Image J software and normalized to the internal control β-actin.

2.7. Quantitative PCR (q-PCR) analysis

Total RNA extraction was performed using the TRIzol reagent (Invitrogen, Carlsbad, CA). All gene mRNA levels were assessed by using individual TaqMan gene expression assays using ABI QuantStudio 3 q-PCR System (Applied Biosystems) following the manufacturer's instructions. The $2^{-\Delta\Delta Ct}$ method was utilized for analyzing relative gene expression levels using human 18S RNA as an internal control [24,25].

2.8. Immunofluorescence (IF) staining

The cultured cells were seeded on a cover glass in a 6-well plate and incubated at 37 °C for 24 or 48 h (including inhibitor treatment). Cells were washed with PBS, fixed with 4% paraformaldehyde for 20 min at room temperature and permeabilized with 1% Triton X-100/PBS for 1.5 min. Then, cells were blocked with 3% bovine serum albumin (BSA)/PBS for 30 min. The primary antibodies were diluted with 1% BSA/PBS (1:200) and incubated at 4 °C overnight, followed by incubation with related secondary antibodies (Alexa Fluor 488 goat anti-rabbit IgG or Alexa Fluor 546 goat anti-mouse IgG, 1:300, Invitrogen) for 1 h at room temperature. At the end of incubation, cells were washed with PBS and stained with 4,6-diamidino-2-phenylindole (DAPI) for 10 min to visualize the nuclei. The fluorescence images were captured and overlaid using the Nikon NIS-Elements software.

2.9. Nude mouse xenograft tumorigenesis studies

Animal protocols for nude mouse xenograft tumorigenesis studies were reviewed and approved by the University of Kentucky Institutional Animal Care and Use Committee. Six-week old female nude mice (Nu/Nu) were purchased from Charles River Laboratory. After one week of acclimation, mice were randomly regrouped with 10 mice in each group. BEAS-2B–As + BaP-Control shRNA, BEAS-2B–As + BaP-ITGA4 shRNA, BEAS-2B–As + BaP-pLenti6.3 or BEAS-2B–As + BaP-pLenti6.3-SUFU were subcutaneously injected into the right flank of nude mice (0.5×10^6 cells in 0.1 mL of 1:1 growth factor-reduced matrigel and PBS). After injection, mice were maintained under specific pathogen-free conditions and monitored weekly for tumor formation and growth. All mice were euthanized 12 weeks after the injection, tumors were dissected from all tumor-bearing mice and fixed in 10% formalin solution for histology analysis.

2.10. Mouse xenograft tumor tissue Ki-67 immunohistochemistry (IHC) staining

Nude mouse xenograft tumor tissue sections were prepared and subjected to Ki-67 IHC staining as described previously [21,26]. The IHC staining images were taken using Nikon NIS-Elements software. Ki67 positive cells (brown) were counted in 30 randomly selected fields per mouse tumor tissue section. All tumors from the ITGA4 knockdown cells and three randomly-selected tumors from the control shRNA cells were analyzed. The quantitated results are presented as the percent of cells with Ki-67 positive staining per field of view per mouse (mean ± SD, n = 30).

2.11. Kaplan-Meier plotter overall survival analysis

The Kaplan–Meier plotter (KM plotter, http://kmplot.com/analysis/) was used to analyze the relationship between the ITGA4 mRNA expression level and overall survival (OS) in lung cancer patients. The expression level cutoff point of the ITGA4 gene were determined according to the upper tertile expression of the gene from the selected lung cancer samples. Non-cigarette smoking patients were excluded.

2.12. Gene correlation analysis in GEPIA

The online database Gene Expression Profiling Interactive Analysis (GEPIA) (http://gepia.cancer-pku.cn/index.html) was used to explore the correlation between ITGA4 and GLI-1 mRNA expression levels in lung adenocarcinoma tissues (LUAD). Gene expression correlation analysis was performed using the given TCGA expression data sets. The Spearman method was used to determine the correlation coefficient. ITGA4 was used for the x-axis, and GLI-1 was represented on the y-axis.

2.13. Gene Set Enrichment Analysis (GSEA)

The transcriptomic profiling data of 519 lung cancer patients (TCGA-LUAD) from the TCGA database were downloaded and used to perform GSEA. GSEA was performed using the software GSEA v4.0.1 (www.broadinstitute.org/gsea). The ITGA4 expression level was dichotomized as low and high categories to annotate phenotype, and KEGG gene sets from MSigDB were chosen as the reference gene sets. All other parameters were set based on their default values.

2.14. Statistical analysis

The statistical analysis of the numerical data (mean ± SD) was performed using SPSS 22.0 (Chicago, IL, USA). The comparisons of different groups were analyzed using Student's t-test or one-way analysis of variance (ANOVA), followed by the least-significant difference post-hoc test when appropriate. The significance of difference in nude mouse tumor incidence rate was analyzed using Fisher's exact test. A p-value of <0.05 was considered statistically significant.

3. Results

3.1. ITGA4 expression levels are significantly up-regulated in arsenic and BaP Co-exposure-transformed cells, which plays an important role in their CSC-like property and tumorigenicity

To further investigate the mechanism by which arsenic and BaP co-exposure acts synergistically in inducing cell transformation, CSC-like property and lung tumorigenicity as reported in our recent study [8], we performed cDNA microarray analysis to identify differentially expressed genes that may play critical roles in the synergistic lung tumorigenic effect of the co-exposure (NCBI GSE149605). ITGA4 is one of the most highly up-regulated genes in the co-exposure-transformed cells. We first performed q-PCR analysis to verify the microarray results and found that ITGA4 mRNA levels are only detected in BaP exposure alone-transformed cells (BEAS-2B–BaP) and the co-exposure-transformed cells (BEAS-2B–As + BaP); but ITGA4 mRNA levels in BEAS-2B–As + BaP are significantly higher than that in BEAS-2B–BaP cells (Fig. 1A). Western blot analysis demonstrated that the ITGA4 protein is only detected in BEAS-2B–BaP and BEAS-2B–As + BaP cells; and ITGA4 protein levels in BEAS-2B–As + BaP are significantly higher than that in BEAS-2B–BaP cells (Fig. 1B). Similarly, the highest ITGA4 levels were also observed in another immortalized human bronchial epithelial cell line 16HBE cells treated with arsenic (1 μM) and BaP (2.5 μM) for 40 weeks (Fig. S1). Interestingly, our recent study showed that only BaP exposure alone or arsenic plus BaP co-exposure is capable of inducing lung tumors in mice and arsenic plus BaP co-exposure causes significantly more lung tumors in mice than BaP exposure alone [8]. Together, these results suggest that ITGA4 up-regulation may play an important role in lung tumorigenesis. This statement is further supported by the Kaplan-Meier analysis of the publicly available microarray data from the KM plotter (http://kmplot.com) showing that higher ITGA4 expression levels in lung cancer patients are associated with a significantly worse overall survival (Fig. 1C).

Next, we sought to determine whether a higher ITGA4 expression level indeed plays a critical role in arsenic and Bap co-exposure-enhanced cell transformation, CSC-like property and tumorigenesis. We stably knocked down ITGA4 expression in BEAS-2B–As + BaP cells. A significant ITGA4 knockdown was confirmed by Western blot analysis (Fig. 1D). The soft agar colony formation assay showed that ITGA4 knockdown cells (BEAS-2B–As + BaP-ITGA4 shRNA) form significantly less soft agar colonies than the control shRNA cells (Fig. 1E), suggesting that ITGA4 knockdown in BEAS-2B–As + BaP cells reduces their transformed phenotype. The suspension culture sphere formation assay revealed that ITGA4 knockdown cells form significantly fewer spheres (Fig. 1F), suggesting that ITGA4 knockdown in BEAS-2B–As + BaP cells greatly reduces their CSC-like property. This statement was further supported by the nude mouse xenograft tumorigenesis study: the tumor incidence rate in mice injected with ITGA4 knockdown cells (2/10 = 20%) was significantly lower than mice injected with control shRNA cells (7/10 = 70%, $p < 0.05$) (Fig. 1G). Moreover, the xenograft tumors formed by injection of the ITGA4 knockdown cells were much smaller than the tumors from injection of control shRNA cells (Fig. 1G). Further tumor histology analysis showed that the proliferation mark Ki-67 positive staining in tumors from ITGA4 knockdown cells is significantly less than the tumors from control

shRNA cells (Fig. 1H). Collectively, these results indicate that ITGA4 up-regulation plays a critical role in the synergistic effect of arsenic and BaP co-exposure in inducing CSC-like property and tumorigenesis.

3.2. The Hedgehog pathway is highly activated in arsenic and BaP Co-exposure-transformed cells and inhibition of the hedgehog pathway significantly reduces their CSC-like property

CSCs or CSC-like cells are considered as tumor initiation cells; and increased CSC-like property enhances tumorigenesis [27,28]. We next wanted to determine how ITGA4 up-regulation enhances the CSC-like property of arsenic and BaP co-exposure-transformed cells. High activation of critical signaling pathways such as the Hedgehog pathway, Notch pathway, and Wnt/β-catenin pathway have been implicated in generating and maintaining CSCs or CSC-like cells [29–32]. We first tested these three major CSC-related pathways (Hedgehog, Notch, and Wnt/β-catenin) to determine if any of them are highly activated in the co-exposure-transformed cells (BEAS-2B–As + Bap). The q-PCR analysis showed that the mRNA level of glioma-associated oncogene homologue-1 (GLI-1), a key signaling effector molecule and the target gene in the Hedgehog pathway, is significantly higher in BEAS-2B–As + BaP cells than that in the passage-matched control cells, arsenic exposure alone-transformed cells (BEAS-2B–As) and BaP exposure alone-transformed cells (BEAS-2B–BaP) (Fig. 2A). In contrast, neither the mRNA level of transcription factor 12 (TCF12), a representative target gene in the Wnt/β-catenin pathway, nor the mRNA level of hairy enhancer of split-1 (HES1), a representative target gene in the Notch pathway, are highest expressed in the BEAS-2B–As + BaP cells (Fig. 2A). These results suggest that the Hedgehog pathway is likely the most activated in the BEAS-2B–As + BaP cells. Subsequent Western blot analysis confirmed that GLI-1 is highly expressed only in BEAS-2B–As + Bap cells. On the contrary, the protein level of SUFU, a negative regulator of GLI-1, is the lowest in BEAS-2B–As + Bap cells (Fig. 2B). The expression levels of other important proteins in the Hedgehog pathway including SHH, Ptch-1 and SMO were not changed dramatically among the four treatment groups of cells (Fig. 2B). Similarly, the highest GLI-1 levels and the lowest SUFU levels were also observed in another immortalized human bronchial epithelial cell line 16HBE cells treated with arsenic (1 μM) and BaP (2.5 μM) for 40 weeks (Fig. S1). GLI-1 is a nuclear-cytoplasmic shuttling protein and its nuclear localization is an indication of its activation [33]. We performed GLI-1 immunofluorescence (IF) staining to determine its cellular localization. As shown in Fig. 2C, GLI-1 positive staining (red signal) was weak and limited in the cytoplasm and nucleus in BEAS-2B-Control and BEAS-2B–As cells; weak and limited GLI-1 nuclear staining was seen in BEAS-2B-Bap cells. However, a significantly stronger GLI-1 nuclear staining (pink signal, GLI-1 staining red signal was overlaid with nuclear DAPI staining blue signal) was observed in BEAS-2B–As + Bap cells. Together, these results suggest that the Hedgehog signaling pathway is strongly activated only in the co-exposure-transformed cells (BEAS-2B–As + Bap).

We then used two approaches to determine whether the highly activated Hedgehog pathway plays a critical role in the enhanced–CSC–like property of the co-exposure-transformed cells (BEAS-2B–As + BaP). First, we treated BEAS-2B–As + BaP cells with Cyclopamine, a small molecule pharmacological inhibitor of the Hedgehog pathway [34]. It was found

that Cyclopamine treatment dose-dependently reduces the GLI-1 protein level (Fig. 2D) and GLI-1 nuclear localization (Fig. 2E) in BEAS-2B–As + BaP cells, indicating that the Hedgehog pathway is efficiently inhibited. In consistence with these findings, Cyclopamine treatment also significantly reduced the capability of BEAS-2B–As + BaP cells in forming suspension culture spheres (Fig. 2F). Secondly, we inhibited the Hedgehog pathway by using the small interference RNA (siRNA) to specifically knock down GLI-1 expression. The significant knockdown of GLI-1 protein levels by GLI-1 siRNA in BEAS-2B–As + BaP cells is shown in Fig. 2G. The suspension culture sphere formation assay showed that GLI-1 knock down significantly reduces the capability of BEAS-2B–As + BaP cells in forming suspension spheres (Fig. 2H). Together, these results indicate that the Hedgehog pathway activation plays an important role in the enhanced–SC–like property of arsenic and BaP co-exposure-transformed cells.

3.3. ITGA4 down-regulation in arsenic and BaP Co-exposure-transformed cells significantly reduces the hedgehog pathway activation by up-regulating SUFU expression levels

We next sought to determine whether knocking down ITGA4 expression levels has an effect on the three aforementioned CSC generating and maintaining pathways. We first used q-PCR analysis to compare the mRNA levels of representative genes activated in the Hedgehog, Wnt/β-catenin or Notch pathways. It was found that ITGA4 knockdown significantly reduces the level of the Hedgehog pathway representative gene GLI-1, but has no significant effect on the levels of TCF12 and HES1 (Fig. 3A), the representative target gene in the Wnt/β-catenin and Notch pathway, respectively. In consistence with the q-PCR analysis results, ITGA4 knockdown also greatly reduced GLI-1 protein levels in BEAS-2B–As + BaP cells (Fig. 3B). Together, these results indicated that ITGA4 knockdown significantly reduces the Hedgehog pathway activation in BEAS-2B–As + BaP cells.

Next, we determined the mechanism of how ITGA4 knockdown reduces the Hedgehog pathway activation in BEAS-2B–As + BaP cells. Western blot analysis revealed that ITGA4 knockdown has no significant effects on the levels of several important proteins in the Hedgehog pathway including SHH, Ptch-1 and SMO (Fig. 3B). However, ITGA4 knockdown greatly increased the protein level of SUFU (Fig. 3B), the central negative regulator of the Hedgehog pathway [35]. Moreover, further IF staining provided additional evidence showing that ITGA4 knockdown increases SUFU protein levels and reduces GLI-1 protein levels and GLI-1 nuclear localization (Fig. 3C). Since SUFU is a negative regulator of the Hedgehog pathway, these results suggest that ITGA4 knockdown reduces the Hedgehog pathway activation and GLI-1 levels likely by increasing the level of SUFU. Indeed, knocking down SUFU in the ITGA4 stable knockdown cells (BEAS-2B–As + BaP-ITGA4 shRNA) greatly increased the level of GLI-1 (Fig. 3D). In addition, the Gene Expression Profiling Interactive Analysis (GEPIA) of the publicly available TCGA expression data showed that GLI-1 expression levels are significantly and positively associated with ITGA4 expression levels in lung cancer (Fig. 3E). Moreover, the Gene Set Enrichment Analysis (GSEA) revealed that the gene sets of the Hedgehog pathway are significantly enriched in lung adenocarcinoma samples from TCGA with high ITGA4

expression (Fig. 3F). Together, these results provided additional evidence supporting that ITGA4 up-regulation leads to the activation of the Hedgehog pathway in arsenic and BaP co-exposure-transformed cells; and that ITGA4 knockdown reduces the Hedgehog pathway activation.

We further determined whether re-activating the Hedgehog pathway in ITGA4 knockdown cells reverses the inhibitory effect of ITGA4 knockdown on the CSC-like property of the co-exposure-transformed cells. We used Purmorphamine to re-activate the Hedgehog pathway in ITGA4 knockdown cells (BEAS-2B–As + BaP-ITGA4 shRNA). Purmorphamine treatment activates the Hedgehog pathway by directly binding and activating SMO [36]. It was found while Purmorphamine treatment does not significantly change SHH, Ptch1, SMO and SUFU protein levels; it dose-dependently increases GLI-1 protein levels in BEAS-2B–As + BaP-ITGA4 shRNA cells (Fig. 3G), indicating the activation of the Hedgehog pathway. As a result, Purmorphamine treatment significantly increased the number of suspension culture spheres formed by BEAS-2B–As + BaP-ITGA4 shRNA cells (Fig. 3H). Collectively, these results suggest that ITGA4 down-regulation in arsenic and BaP co-exposure-transformed cells reduces their CSC-like property and tumorigenicity mainly by inhibiting the Hedgehog pathway through increasing its negative regulator SUFU protein level.

3.4. Stably overexpressing SUFU in arsenic and BaP Co-exposure-transformed cells significantly reduces the hedgehog pathway activation, CSC-like property and tumorigenicity

To further demonstrate the important role of SUFU down-regulation in the Hedgehog pathway activation and the CSC-like property and the tumorigenicity of arsenic and BaP co-exposure-transformed cells, we stably overexpressed SUFU in the co-exposure-transformed cells. SUFU overexpression was confirmed by Western blot analysis (Fig. 4A). SUFU overexpression greatly reduced the level of GLI-1 compared to the vector control cells (BEAS-2B–As + BAP-pLenti6.3) (Fig. 4A). However, SUFU overexpression had no effects on the levels of SHH and Ptch-1 proteins, and only slightly reduced SMO protein levels (Fig. 4A).

The soft agar colony formation assay showed that BEAS-2B–As + BaP cells with SUFU overexpression formed significantly less colonies than the vector control cells (Fig. 4B), suggesting that SUFU overexpression in the co-exposure-transformed cells significantly reduces their transformed phenotype. Moreover, the serum-free suspension culture sphere formation assay showed that SUFU overexpression cells formed significantly fewer suspension spheres than the vector control cells (Fig. 4C), suggesting that SUFU overexpression in the co-exposure-transformed cells greatly reduces their CSC-like property. This statement is further supported by the results from nude mouse xenograft tumorigenesis experiment: the tumor incidence rate in mice injected with SUFU overexpression cells (2/10 = 20%) was significantly lower than mice injected with vector control cells (7/10 = 70%, $p < 0.05$) (Fig. 4D). Together, these results indicate that SUFU down-regulation in arsenic and BaP co-exposure-transformed cells plays a critical role in their enhanced CSC-like property and tumorigenicity. Moreover, they also suggest that SUFU up-regulation in ITGA4

knockdown cells (BEAS-2B–As + BaP-ITGA4 shRNA) plays an important role in their reduced CSC-like property and tumorigenicity.

3.5. ITGA4 down-regulation in arsenic and BaP Co-exposure-transformed cells up-regulates SUFU levels by increasing SUFU protein stability

The previous results demonstrated that (i) SUFU up-regulation in the co-exposure-transformed cells with ITGA4 stable knockdown plays an important role in the inhibitory effect of ITGA4 knockdown on their CSC-like property and tumorigenicity (Fig. 3); and (ii) stably overexpressing SUFU in the co-exposure-transformed cells significantly reduces their CSC-like property and tumorigenicity (Fig. 4). We then began to determine the mechanism by which ITGA4 knockdown up-regulates SUFU expression levels in the co-exposure-transformed cells. In other words, we wanted to determine the mechanism of how ITGA4 up-regulation greatly reduces SUFU expression levels in the co-exposure-transformed cells. We first performed q-PCR analysis and determined that no significant differences of SUFU mRNA levels are observed between BEAS-2B–As + Bap-Control shRNA and BEAS-2B–As + Bap-ITGA4 shRNA cells (Fig. 5A). These results suggest that ITGA4 knockdown has no significant effects on SUFU gene transcription. We next determined whether ITGA4 knockdown has an effect on SUFU protein stability by performing cycloheximide (CHX) chase analysis to compare SUFU protein degradation rates in BEAS-2B–As + BaP-Control shRNA and BEAS-2B–As + BaP-ITGA4 shRNA cells. CHX is a chemical inhibitor of protein translation and CHX treatment blocks new protein synthesis, allowing the determination of the effect of proteasome degradation on protein levels [37]. It was found that SUFU protein levels are rapidly decreased in control shRNA cells with the extension of CHX treatment time (Fig. 5B). In contrast, SUFU protein levels are only slightly decreased in ITGA4 knockdown cells with the extension of CHX treatment time (Fig. 5B–C). These results indicate that ITGA4 knockdown in the co-exposure-transformed cells significantly increases SUFU protein stability. In other words, ITGA4 up-regulation in the co-exposure-transformed cells down-regulates SUFU protein levels by reducing SUFU protein stability. To support these statements, the proteasome degradation inhibitor MG132 treatment experiments were performed. It was found that MG132 treatment greatly recovers SUFU protein levels in BEAS-2B–As + Bap-Control shRNA cells, resulting in similar SUFU protein levels in control shRNA cells compared to those of BEAS-2B–As + Bap-ITGA4 shRNA cells (Fig. 5D). Together, these results indicate that ITGA4 knockdown in the co-exposure-transformed cells up-regulates SUFU protein levels by increasing SUFU protein stability and reducing its proteasome degradation.

3.6. ITGA4 down-regulation in arsenic and BaP Co-exposure-transformed cells reduces the PI3K/Akt Pathway Activity to increase SUFU protein stability

We further elucidated the mechanism of how ITGA4 knockdown in arsenic and BaP co-exposure-transformed cells increases SUFU protein stability. Previous studies reported that the Hedgehog pathway can be activated by the PI3K/Akt and Ras/Raf/Mek/Erk signaling to increase GLI protein stability [38,39]. Our recent study revealed a significantly strong activation of Akt and Erk1/2 in BEAS-2B–As + Bap cells, and Akt activation plays an important role in the enhanced–SC–like property of the co-exposure-transformed cells [8]. We sought to determine whether ITGA4 down-regulation in the co-exposure-

transformed cells inhibits Akt or Erk1/2 activity to increase SUFU protein stability and reduce the Hedgehog pathway activation. We first examined whether ITGA4 knockdown in the co-exposure-transformed cells has any effect on Akt and Erk1/2 activation. Western blot analysis showed that the phosphor-Akt (p-Akt) level is greatly reduced in ITGA4 knockdown cells although the phosphor-Erk1/2 (p-Erk1/2) level remains unchanged (Fig. 6A). Given the critical role of Akt activation in the enhanced–CSC–like property of the co-exposure-transformed cells [8], these results suggest that ITGA4 knockdown increases SUFU protein stability and reduces GLI-1 protein levels to impair the co-exposure-transformed cells' CSC-like property likely by reducing Akt activation. To support this statement, we treated the co-exposure-transformed cells with a PI3K inhibitor Wortmannin. Western blot analysis revealed that Wortmannin treatment greatly reduces p-Akt levels, and increases SUFU but decreases GLI-1 protein levels (Fig. 6B). These results are supported by IF staining, which show that Wortmannin treatment greatly increases SUFU protein levels and reduces GLI-1 protein levels and nuclear localization (Fig. 6C).

We next performed the CHX chase experiment to determine whether Wortmannin treatment has an effect on SUFU protein stability. Similar to the results shown in Fig. 5B, the SUFU protein level decreased rapidly with the extension of CHX treatment time in the co-exposure-transformed cells (Fig. 6D). In contrast, the SUFU protein level remained largely unchanged when the co-exposure-transformed cells were pre-treated with Wortmannin plus the same CHX treatment (Fig. 6D). These results indicate that inhibition of the PI3K/Akt pathway greatly increases SUFU protein stability in the co-exposure-transformed cells.

To further demonstrate that the increase of SUFU protein stability in ITGA4 knockdown cells is indeed due to the reduced Akt activity or phosphor-Akt level, we treated ITGA4 knockdown cells with a protein phosphatase inhibitor Okadaic acid (OA) to restore phosphor-Akt levels and determined its effect on SUFU and GLI-1 protein levels. It was found that OA treatment dose-dependently recovers phosphor-Akt levels in ITGA4 knockdown cells, and at the same time, dose-dependently reduces SUFU protein levels and increases GLI-1 protein levels (Fig. 6E). Moreover, treatment with the proteasome degradation inhibitor MG132 completely reversed the effect of OA treatment on SUFU and GLI-1 proteins: MG132 treatment prevented the OA treatment-caused SUFU decrease and GLI-1 increase (Fig. 6E). We understand that OA treatment is capable of increasing many protein phosphor-levels [40]. Next, we specifically inhibited Akt activity in OA-treated ITGA4 knockdown cells to further confirm the role of Akt activity in this process. As shown in Fig. 6F, when ITGA4 knockdown cells were treated with OA plus an Akt specific inhibitor, the effect of OA treatment in decreasing SUFU and increasing GLI-1 protein levels was overcome by the Akt inhibitor co-treatment. Collectively, these results indicate that ITGA4 knockdown in the co-exposure-transformed cells increases SUFU and decreases GLI-1 protein levels by reducing the PI3K/Akt pathway activity.

4. Discussion

Studies, including ours, have shown that arsenic and BaP co-exposure acts synergistically in inducing cell transformation, CSC-like property and tumorigenesis [6–8,41]; however, the underlying mechanism has not been well understood. Given the wide presence of arsenic

and BaP in water and food, and the popularity of cigarette smoking in many regions, human co-exposure to arsenic and BaP could be common. Arsenic and BaP co-exposure could have significantly more harmful effects on human health than the effects caused by arsenic or BaP exposure alone. It is imperative to investigate the mechanism of the synergistic adverse health effects of arsenic and BaP co-exposure. In this study, we demonstrated that arsenic and BaP co-exposure greatly up-regulates the expression of ITGA4, which in turn activates the Hedgehog pathway to enhance arsenic and BaP co-exposure-induced CSC-like property and tumorigenesis (see Fig. 7).

Integrin family members have been shown to play important roles in tumor metastasis [9]; however, little evidence is available to show that integrins are critically involved in environmental carcinogen-induced cell malignant transformation and tumorigenesis. ITGA4 is one of the least studied integrins [10]. Studies have shown that ITGA4 plays important roles in mediating cell-cell and cell-matrix adhesion as well as regulating cell migration and invasion [10]. Like other integrin family members, ITGA4 has also been shown to play important roles in tumor metastasis [11]. However, whether ITGA4 plays a role in cell malignant transformation and the tumor development process is unknown. This study provides the first evidence showing that environmental exposure such as arsenic and BaP co-exposure up-regulates the expression of ITGA4, which plays a crucial role in the co-exposure-induced CSC-like property and tumorigenesis. Given the important role of ITGA4 in tumor development as demonstrated in this study and its importance in tumor metastasis as demonstrated by other studies [11], further studies are needed to determine how ITGA4 expression levels are up-regulated. Understanding the mechanism of ITGA4 up-regulation by arsenic and BaP co-exposure may identify additional targets for the prevention and treatment of lung cancer resulting from arsenic and BaP co-exposure.

The Hedgehog pathway is one of the highly conserved and key development pathways, playing important roles in normal embryonic development [13]. On the contrary, high activation of the Hedgehog pathway during the adult stage has been shown to be critically involved in cancer metastasis and therapeutic resistance [13,42]. However, whether environmental carcinogen exposure activates the Hedgehog pathway and whether the Hedgehog pathway activation plays an important role in environmental carcinogenesis remain largely unknown. In this study, we provided the first evidence showing that although arsenic or BaP exposure alone does not activate the Hedgehog pathway, in sharp contrast, arsenic and BaP co-exposure causes a strong activation of the Hedgehog pathway. Moreover, we further determined that Hedgehog pathway activation plays a critical role in arsenic and BaP co-exposure-induced CSC-like property and tumorigenesis. These findings not only offer new insight for understanding the mechanism of the synergistic lung tumorigenic effect of arsenic and BaP co-exposure, but also suggest that the Hedgehog pathway may serve as an important target for the prevention and treatment of lung cancer resulting from arsenic and BaP co-exposure.

How does arsenic and BaP co-exposure activate the Hedgehog pathway? In general, the Hedgehog pathway is activated by the binding of the Hedgehog ligand to its transmembrane receptor Ptch leading to the de-repression of SMO and subsequent activation of GLI transcription factors, which is also known as the canonical Hedgehog pathway [16, 43].

On the other hand, the Hedgehog pathway can also be activated independent of its ligand-receptor interaction-mediated SMO de-repression, which is termed as the non-canonical Hedgehog pathway [38,39]. Several mechanisms have been proposed for the non-canonical Hedgehog pathway activation including Kras signaling, PI3K/Akt signaling, transforming growth factor β signaling, protein kinase C signaling, etc. [38,39]. In this study, we demonstrated that arsenic and BaP co-exposure causes a non-canonical Hedgehog pathway activation via the PI3K/Akt signaling. This finding is consistent with our recent report showing that arsenic and BaP co-exposure cause a strong activation of Akt, which plays a critical role in the co-exposure-enhanced CSC-like property and tumorigenesis [8]. Moreover, the finding that arsenic and BaP co-exposure activates the Hedgehog pathway via the PI3K/Akt signaling also provides new mechanistic insight for understanding how Akt activation enhances the co-exposure-induced CSC-like property and tumorigenesis.

How does the PI3K/Akt signaling activate the Hedgehog pathway in arsenic and BaP co-exposure-transformed cells? The non-canonical Hedgehog pathway activation is mostly observed in cancer cells. The first evidence showing the involvement of the PI3K/Akt signaling in the Hedgehog pathway activation was from Riobó N et al. reporting that Akt prevents proteasomal degradation of GLI-2 [44]. Other studies have shown that the AKT signaling increases GLI-1 protein stability and GLI-1 transcriptional activity [45,46]. In this study, we demonstrated that the PI3K/Akt signaling activates the Hedgehog pathway by reducing the level of the Hedgehog pathway's negative regulator SUFU leading to GLI-1 activation. It was determined that the Akt signaling reduces SUFU protein levels by reducing its protein stability and promoting its proteasome degradation. Further studies are needed to determine how the PI3K/Akt signaling reduces SUFU protein stability.

BEAS-2B cells are immortalized human bronchial epithelial cells and grow well in the presence of serum. It was reported that BEAS-2B cells cultured in 5% FBS for 8 weeks are almost 5 times more sensitive to arsenite (2 μM and above) cytotoxicity than BEAS-2B cells cultured in the absence of FBS [47]. This finding suggests that culturing BEAS-2B cells with or without FBS could affect BEAS-2B cells' responses to toxicant exposures and it is important to culture BEAS-2B cells under the same conditions when using BEAS-2B cells as a model to study the toxic effects of toxicant exposures. In this study, we used arsenite (1 μM) and/or BaP (2.5 μM) exposure-transformed BEAS-2B cells generated in our recent study [8]. No further arsenite and/or BaP exposure was carried out in this study. Moreover, we included passage-matched control BEAS-2B cells as a proper control group in our study. All groups of BEAS-2B cells were cultured under the same conditions with the presence of 5% FBS, which will not likely have a significant impact on the toxic effects of arsenic and BaP exposure reported here.

In summary, this study demonstrates that ITGA4 up-regulation activates the Hedgehog pathway, which plays an important role in arsenic and BaP co-exposure-induced CSC-like property and tumorigenesis. These findings not only offer new insight for understanding the mechanism of the synergistic carcinogenic effect of arsenic and BaP co-exposure, but also provide the first evidence showing that the Hedgehog pathway effector GLI-1 is a critical mediator of the ITGA4 tumorigenic signaling.

Supplementary Material

Refer to Web version on PubMed Central for supplementary material.

Acknowledgments

This work was supported by National Institute of Health grant 1R01ES028256 to Z.W. This research was also supported by the Shared Biospecimen Procurement and Translational Pathology Core Facility at the University of Kentucky Markey Cancer Center (P30CA177558). We thank Mr. Yuquan Bai (Department of Thoracic Surgery research laboratory, West China Hospital, Sichuan University, Chengdu, Sichuan, P.R. China) for his kind assistance in bioinformatics analysis.

References

[1]. Tsiaoussis J, Antoniou MN, Koliarakis I, Mesnage R, Vardavas CI, Izotov BN, Psaroulaki A, Tsatsakis A, Effects of single and combined toxic exposures on the gut microbiome: current knowledge and future directions, Toxicol. Lett 312 (2019) 72–97. [PubMed: 31034867]

[2]. Zhou F, Yin G, Gao Y, Liu D, Xie J, Ouyang L, Fan Y, Yu H, Zha Z, Wang K, Shao L, Feng C, Fan G, Toxicity assessment due to prenatal and lactational exposure to lead, cadmium and mercury mixtures, Environ. Int 133 (2019) 105192. [PubMed: 31639605]

[3]. Bellavia A, James-Todd T, Williams PL, Approaches for incorporating environmental mixtures as mediators in mediation analysis, Environ. Int 123 (2019) 368–374. [PubMed: 30572168]

[4]. Bopp SK, Barouki R, Brack W, Dalla Costa S, Dorne J-LCM, Drakvik PE, Faust M, Karjalainen TK, Kephalopoulos S, van Klaveren J, Kolossa-Gehring M, Kortenkamp A, Lebret E, Lettieri T, Nørager S, Rüegg J, Tarazona JV, Trier X, van de Water B, van Gils J, Bergman Å, Current EU research activities on combined exposure to multiple chemicals, Environ. Int 120 (2018) 544–562. [PubMed: 30170309]

[5]. IARC, Some drinking-water disinfectants and contaminants, including arsenic, IARC Monogr. Eval. Carcinog. Risks Hum 84 (2004) 1–477. [PubMed: 15645577]

[6]. Ishinishi N, Kodama Y, Nobutomo K, Hisanaga A, Preliminary experimental study on carcinogenicity of arsenic trioxide in rat lung, Environ. Health Perspect 19 (1977) 191–196. [PubMed: 908298]

[7]. Pershagen G, Nordberg G, Björklund N-E, Carcinomas of the respiratory tract in hamsters given arsenic trioxide and/or benzo [a] pyrene by the pulmonary route, Environ. Res 34 (1984) 227–241. [PubMed: 6086305]

[8]. Wang Z, Yang P, Xie J, Lin HP, Kumagai K, Harkema J, Yang C, Arsenic and benzo[α]pyrene co-exposure acts synergistically in inducing cancer stem cell-like property and tumorigenesis by epigenetically down-regulating SOCS3 expression, Environ. Int 137 (2020) 105560. [PubMed: 32062438]

[9]. Hamidi H, Ivaska J, Every step of the way: integrins in cancer progression and metastasis, Nat. Rev. Drug Discov 17 (2018) 31–46.

[10]. Hight-Warburton W, Parsons M, Regulation of cell migration by α4 and α9 integrins, Biochem. J 476 (2019) 705–718. [PubMed: 30819933]

[11]. Schlesinger M, Bendas G, Contribution of very late antigen-4 (VLA-4) integrin to cancer progression and metastasis, Canc. Metastasis Rev 34 (2015) 575–591.

[12]. Jiang J, Hui C.-c., Hedgehog signaling in development and cancer, Dev. Cell 15 (2008) 801–812. [PubMed: 19081070]

[13]. Jeng K-S, Chang C-F, Lin S-S, Sonic hedgehog signaling in organogenesis, tumors, and tumor microenvironments, Int. J. Mol. Sci 21 (2020) 758.

[14]. Qi X, Li X, Mechanistic insights into the generation and transduction of hedgehog signaling, Trends Biochem. Sci 45 (2020) 397–410. [PubMed: 32311334]

[15]. Carballo GB, Honorato JR, de Lopes GPF, A highlight on Sonic hedgehog pathway, Cell Commun. Signal 16 (2018) 11. [PubMed: 29558958]

[16]. Robbins DJ, Fei DL, Riobo NA, The Hedgehog signal transduction network, Sci. Signal 5 (2012) re6. [PubMed: 23074268]

[17]. Methot N, Basler K, Suppressor of Fused Opposes Hedgehog Signal Transduction by Impeding Nuclear Accumulation of the Activator Form of Cubitus Interruptus, vol. 127, Development, Cambridge, England), 2000, pp. 4001–4010. [PubMed: 10952898]

[18]. Wang Z, Li Y, Xiao Y, Lin H-P, Yang P, Humphries B, Gao T, Yang C, Integrin α9 depletion promotes β-catenin degradation to suppress triple-negative breast cancer tumor growth and metastasis, Int. J. Canc 145 (2019) 2767–2780.

[19]. Yang C, Wu J, Zhang R, Zhang P, Eckard J, Yusuf R, Huang X, Rossman TG, Frenkel K, Caffeic acid phenethyl ester (CAPE) prevents transformation of human cells by arsenite (As) and suppresses growth of As-transformed cells, Toxicology 213 (2005) 81–96. [PubMed: 16085347]

[20]. Wang Z, Lin H-P, Li Y, Tao H, Yang P, Xie J, Maddy D, Kondo K, Yang C, Chronic hexavalent chromium exposure induces cancer stem cell-like property and tumorigenesis by increasing c-myc expression, Toxicol. Sci 172 (2019) 252–264. [PubMed: 31504995]

[21]. Humphries B, Wang Z, Li Y, Jhan JR, Jiang Y, Yang C, ARHGAP18 downregulation by miR-200b suppresses metastasis of triple-negative breast cancer by enhancing activation of RhoA, Canc. Res 77 (2017) 4051–4064.

[22]. Wang Z, Humphries B, Xiao H, Jiang Y, Yang C, Epithelial to mesenchymal transition in arsenic-transformed cells promotes angiogenesis through activating β-catenin–vascular endothelial growth factor pathway, Toxicol. Appl. Pharmacol 271 (2013) 20–29. [PubMed: 23643801]

[23]. Wang Z, Humphries B, Xiao H, Jiang Y, Yang C, MicroRNA-200b suppresses arsenic-transformed cell migration by targeting protein kinase Calpha and Wnt5b-protein kinase Calpha positive feedback loop and inhibiting Rac1 activation, J. Biol. Chem 289 (2014) 18373–18386. [PubMed: 24841200]

[24]. Wang Z, Zhao Y, Smith E, Goodall GJ, Drew PA, Brabletz T, Yang C, Reversal and prevention of arsenic-induced human bronchial epithelial cell malignant transformation by microRNA-200b, Toxicol. Sci.: Off. J. Soc. Toxicol 121 (2011) 110–122.

[25]. Xiao Y, Li Y, Tao H, Humphries B, Li A, Jiang Y, Yang C, Luo R, Wang Z, Integrin alpha5 down-regulation by miR-205 suppresses triple negative breast cancer stemness and metastasis by inhibiting the Src/Vav2/Rac1 pathway, Canc. Lett 433 (2018) 199–209.

[26]. Humphries B, Wang Z, Oom AL, Fisher T, Tan D, Cui Y, Jiang Y, Yang C, MicroRNA-200b targets protein kinase Calpha and suppresses triple-negative breast cancer metastasis, Carcinogenesis 35 (2014) 2254–2263. [PubMed: 24925028]

[27]. Najafi M, Farhood B, Mortezaee K, Cancer stem cells (CSCs) in cancer progression and therapy, J. Cell. Physiol 234 (2019) 8381–8395. [PubMed: 30417375]

[28]. Heng WS, Gosens R, Kruyt FAE, Lung cancer stem cells: origin, features, maintenance mechanisms and therapeutic targeting, Biochem. Pharmacol 160 (2019) 121–133. [PubMed: 30557553]

[29]. Nusse R, Clevers H, Wnt/β-catenin signaling, disease, and emerging therapeutic modalities, Cell 169 (2017) 985–999. [PubMed: 28575679]

[30]. Matsui WH, Cancer stem cell signaling pathways, Medicine (2016) 95. [PubMed: 27334457]

[31]. Takebe N, Miele L, Harris PJ, Jeong W, Bando H, Kahn M, Yang SX, Ivy SP, Targeting Notch, Hedgehog, and Wnt pathways in cancer stem cells: clinical update, Nat. Rev. Clin. Oncol 12 (2015) 445. [PubMed: 25850553]

[32]. Milla LA, González-Ramírez CN, Palma V, Sonic Hedgehog in cancer stem cells: a novel link with autophagy, Biol. Res 45 (2012) 223–230. [PubMed: 23283432]

[33]. Kogerman P, Grimm T, Kogerman L, Krause D, Undén AB, Sandstedt B, Toftgård R, Zaphiropoulos PG, Mammalian Suppressor-of-Fused modulates nuclear–cytoplasmic shuttling of GLI-1, Nat. Cell Biol 1 (1999) 312–319. [PubMed: 10559945]

[34]. Binder M, Chmielarz P, McKinnon PJ, Biggs LC, Thesleff I, Balic A, Functionally distinctive Ptch receptors establish multimodal hedgehog signaling in the tooth epithelial stem cell niche, Stem cells (Dayton, Ohio) 37 (2019) 1238–1248.

[35]. Gonnissen A, Isebaert S, Haustermans K, Targeting the Hedgehog signaling pathway in cancer: beyond Smoothened, Oncotarget 6 (2015) 13899. [PubMed: 26053182]

[36]. Stanton BZ, Peng LF, Small-molecule modulators of the Sonic Hedgehog signaling pathway, Mol. Biosyst 6 (2010) 44–54. [PubMed: 20024066]

[37]. Buchanan BW, Lloyd ME, Engle SM, Rubenstein EM, Cycloheximide chase analysis of protein degradation in Saccharomyces cerevisiae, JoVE (2016), e53975.

[38]. Pietrobono S, Gagliardi S, Stecca B, Non-canonical hedgehog signaling pathway in cancer: activation of GLI transcription factors beyond smoothened, Front. Genet 10 (2019) 556. [PubMed: 31244888]

[39]. Gu D, Xie J, Non-canonical Hh signaling in cancer—current understanding and future directions, Cancers 7 (2015) 1684–1698. [PubMed: 26343727]

[40]. Haystead TA, Sim AT, Carling D, Honnor RC, Tsukitani Y, Cohen P, Hardie DG, Effects of the tumour promoter okadaic acid on intracellular protein phosphorylation and metabolism, Nature 337 (1989) 78–81. [PubMed: 2562908]

[41]. Pang Y, Xu Y, Li H, Li Y, Zhao Y, Jiang R, Shen L, Zhou J, Wang X, Liu Q, The inhibition of HIF-2α on the ATM/Chk-2 pathway is involved in the promotion effect of arsenite on benzo (a) pyrene-induced cell transformation, Toxicol. Lett 218 (2013) 105–117. [PubMed: 23333640]

[42]. Giroux-Leprieur E, Costantini A, Ding VW, He B, Hedgehog signaling in lung cancer: from oncogenesis to cancer treatment resistance, Int. J. Mol. Sci 19 (2018) 2835.

[43]. Briscoe J, Thérond PP, The mechanisms of Hedgehog signalling and its roles in development and disease, Nat. Rev. Mol. Cell Biol 14 (2013) 416–429. [PubMed: 23719536]

[44]. Riobó NA, Lu K, Ai X, Haines GM, Emerson CP, Phosphoinositide 3-kinase and Akt are essential for sonic hedgehog signaling, Proc. Natl. Acad. Sci. Unit. States Am 103 (2006) 4505–4510.

[45]. Stecca B, Mas C, Clement V, Zbinden M, Correa R, Piguet V, Beermann F, i Altaba AR, Melanomas require HEDGEHOG-GLI signaling regulated by interactions between GLI1 and the RAS-MEK/AKT pathways, Proc. Natl. Acad. Sci. Unit. States Am 104 (2007) 5895–5900.

[46]. Singh R, Dhanyamraju PK, Lauth M, DYRK1B blocks canonical and promotes non-canonical Hedgehog signaling through activation of the mTOR/AKT pathway, Oncotarget 8 (2017) 833. [PubMed: 27903983]

[47]. Zhao F, Klimecki WT, Culture conditions profoundly impact phenotype in BEAS-2B, a human pulmonary epithelial model, J. Appl. Toxicol 35 (2015) 945–951. [PubMed: 25524072]

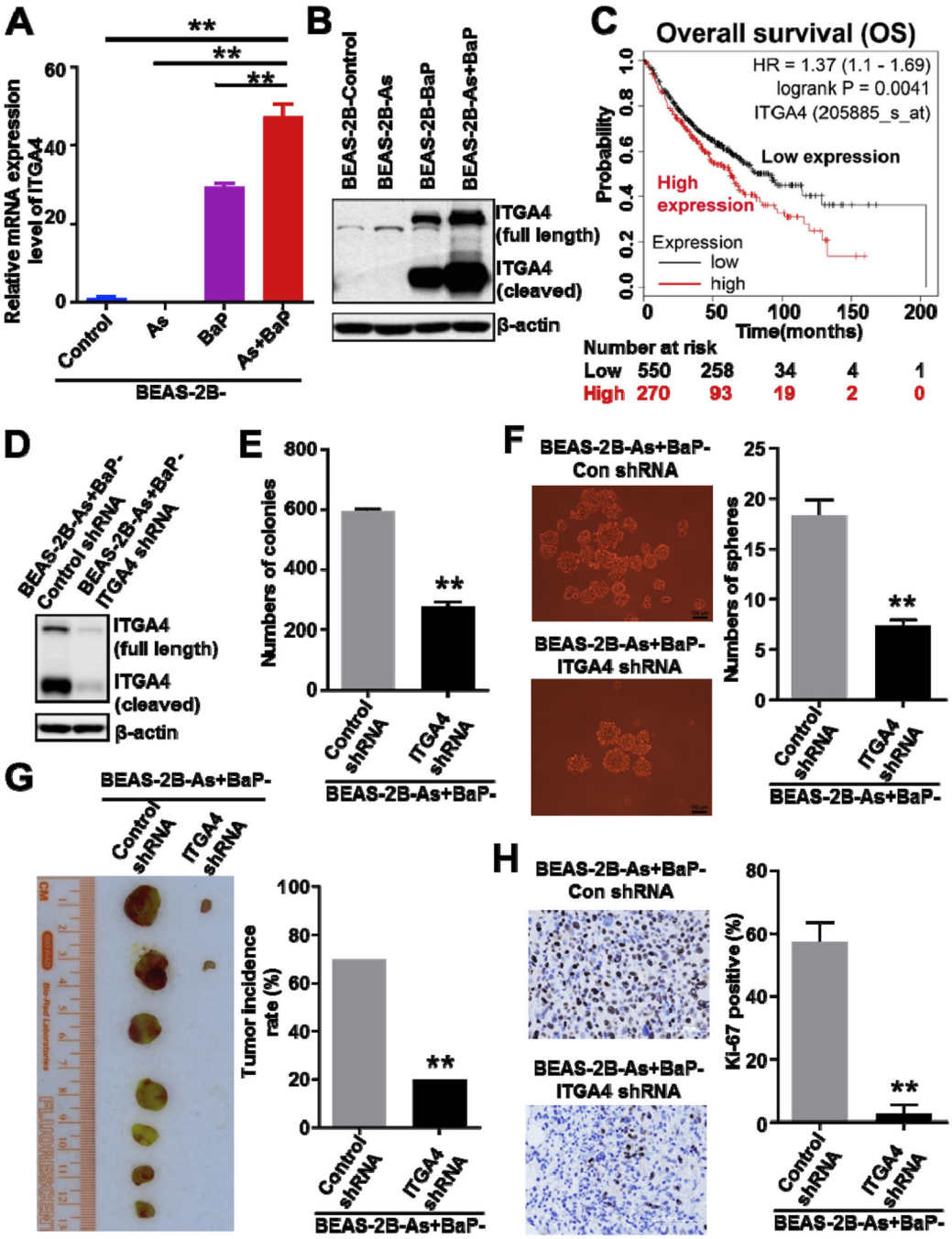

Fig. 1.

ITGA4 expression levels are significantly up-regulated in arsenic and BaP co-exposure-transformed cells and down-regulation of ITGA4 levels significantly reduce their CSC-like property and tumorigenicity. (A) Q-PCR analysis of the relative mRNA levels of ITGA4 in passage-matched control cells (BEAS-2B-Control), arsenic exposure alone-transformed cells (BEAS-2B–As), BaP exposure alone-transformed cells (BEAS-2B–BaP) and arsenic plus BaP co-exposure-transformed cells (BEAS-2B–As + BaP). The ITGA4 mRNA levels are expressed relative to BEAS-2B-Control cells (mean ± SD, n = 3). **

$p < 0.01$. (B) Representative Western blot analysis of ITGA4 protein levels in BEAS-2B-Control, BEAS-2B–As, BEAS-2B–BaP and BEAS-2B–As + BaP cells. Similar results were obtained in the repeated Western blots. (C) The KM plotter analysis of the relationship between ITGA4 gene expression levels and overall survival in lung cancer patients. (D) Representative Western blot analysis of ITGA4 protein levels in arsenic and BaP co-exposure-transformed cells stably expressing a non-targeting control shRNA (BEAS-2B–As + BaP-Control shRNA) or ITGA4 specific targeting shRNA (BEAS-2B–As + BaP-ITGA4 shRNA). Similar results were observed in the repeated Western blots. (E–F) Effect of stably knocking down ITGA4 expression in arsenic and BaP co-exposure-transformed cells on their capability of forming soft agar colonies (E) and suspension culture spheres (F) (mean ± SD, n = 3). ** $p < 0.01$, compared to BEAS-2B–As + BaP-Control shRNA cells. (G–H) Mouse xenograft tumor images, tumor incidence rate (G) and representative tumor tissue section Ki-67 IHC staining with the quantitative results of Ki-67 positive staining (mean ± SD, n = 30) (H). * $p < 0.05$, ** $p < 0.01$ compared to tumors from injection of control shRNA cells.

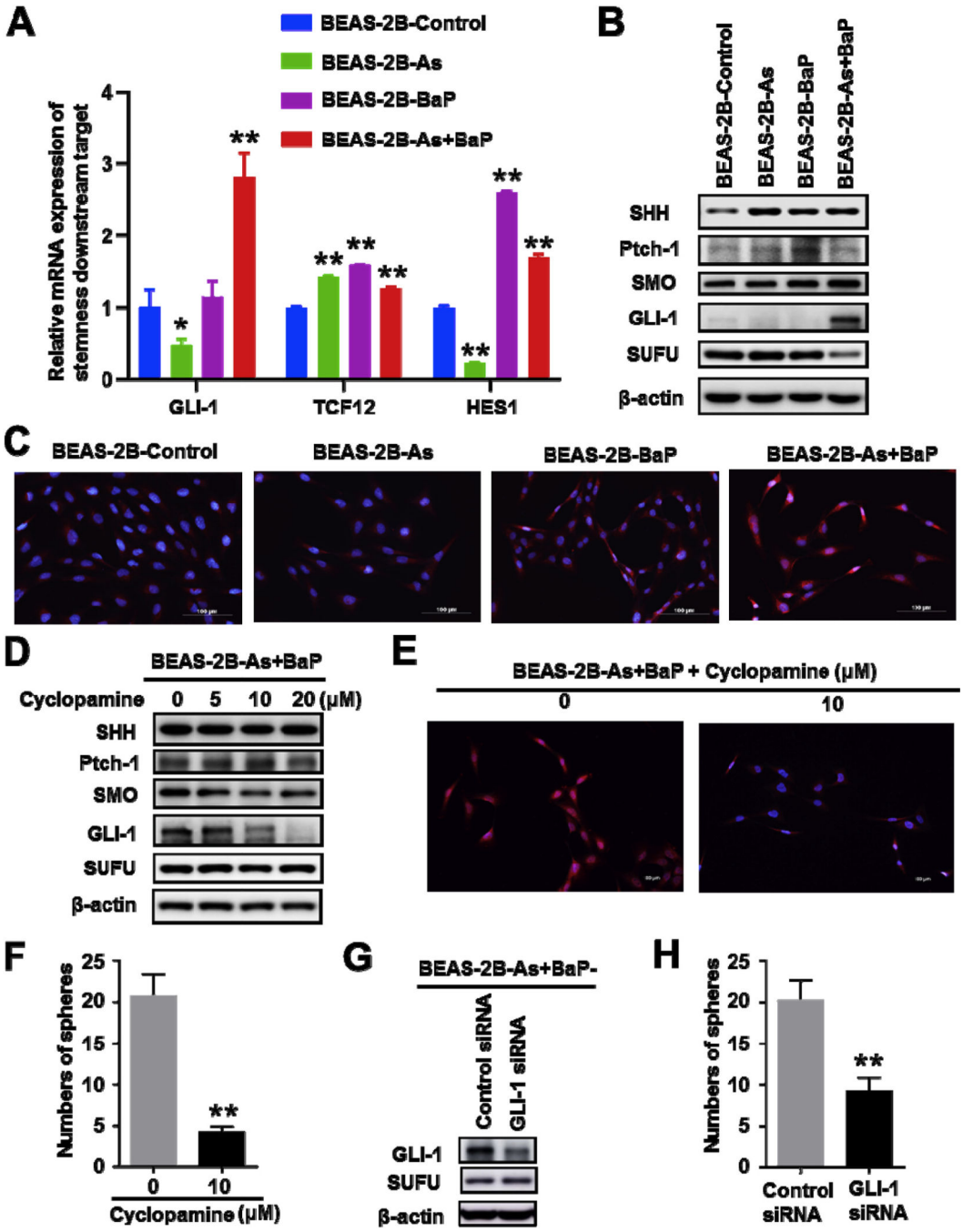

Fig. 2.

The Hedgehog pathway is highly activated in arsenic and BaP co-exposure-transformed cells and inhibiting the Hedgehog pathway significantly reduces their CSC-like property. (A) Q-PCR analysis of the relative mRNA expression levels of GLI-1, TCF12 and HES1 in passage-matched control cells (BEAS-2B-Control), arsenic exposure alone-transformed cells (BEAS-2B–As), BaP exposure alone-transformed cells (BEAS-2B–BaP) and arsenic plus BaP co-exposure-transformed cells (BEAS-2B–As + BaP). The mRNA levels are expressed relative to BEAS-2B-Control cells (mean ± SD, n = 3). ** $p < 0.01$, compared

to BEAS-2B-Control cells. (B) Representative Western blot analysis of the expression levels of SHH, Ptch-1, SMO, SUFU and GLI-1 protein in BEAS-2B-Control, BEAS-2B–As, BEAS-2B–BaP and BEAS-2B–As + BaP. (C) Representative IF staining overlaid images of GLI-1 staining in red fluorescence with nuclear DAPI staining in blue fluorescence. Scale bar: 100 μm. (D) Representative western blot analysis of the effects of different concentrations of Cyclopamine (0, 5, 10, 20 μM) treatment (24 h) on the Hedgehog pathway protein expression levels in BEAS-2B–As + BaP cells. (E) Representative IF staining overlaid images of GLI-1 staining in red fluorescence with nuclear DAPI staining in blue fluorescence. Scale bar: 100 μm. (F) Effect of Cyclopamine treatment on suspension culture spheres formation of BEAS-2B–As + BaP cells (mean ± SD, n = 3). ** $p < 0.01$, compared to vehicle control-treated cells. (G) Representative Western blot analysis of GLI-1, SUFU protein levels in BEAS-2B–As + BaP cells transfected with Control siRNA (Con siRNA) or GLI-1 siRNA. (H) Effect of knocking down GLI-1 expression levels in BEAS-2B–As + BaP cells on their capability of forming suspension culture spheres (mean ± SD, n = 3). ** $p < 0.01$, compared to control siRNA-transfected cells. Similar results were obtained in the repeated experiments.

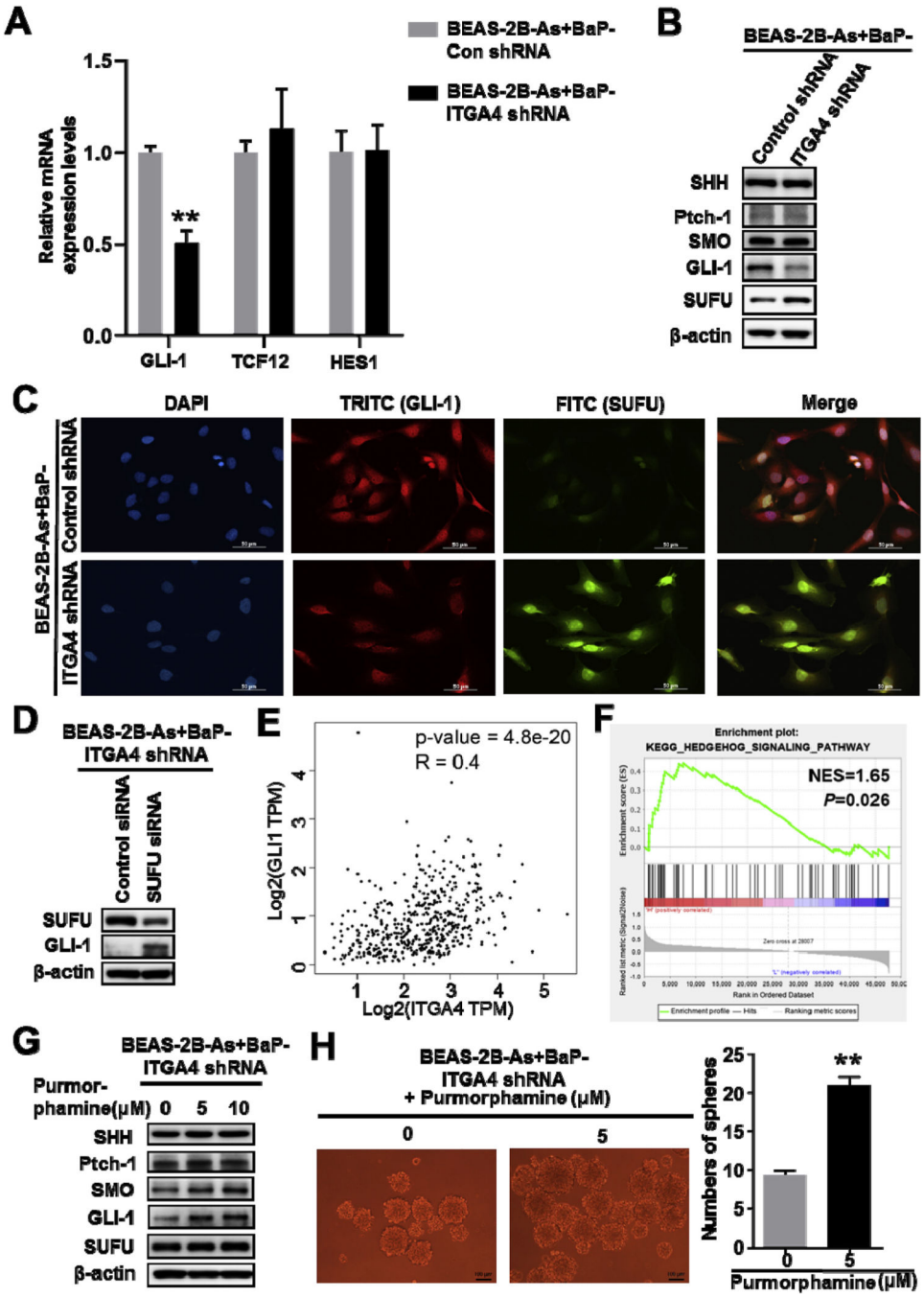

Fig. 3.

ITGA4 down-regulation in arsenic and BaP co-exposure-transformed cells significantly reduces the Hedgehog pathway activation by up-regulating SUFU expression level. (A) Q-PCR analysis of mRNA levels of GLI-1, TCF12, and HES1 in shRNA vector control and ITGA4 stable knockdown BEAS-2B–As + BaP cells. (B) Representative Western blot analysis of SHH, Ptch-1, SMO, SUFU and GLI-1 protein levels in shRNA vector control and ITGA4 stable knockdown BEAS-2B–As + BaP cells. Similar results were obtained in the repeated experiments. (C) Representative IF staining images and overlaid images

of GLI-1 staining in red fluorescence, SUFU staining in green fluorescence and nuclear DAPI staining in blue fluorescence. Scale bar: 50 μm. Similar results were obtained in the repeated experiments. (D) Representative Western blot analysis of GLI-1 and SUFU protein levels in BEAS-2B–As + BaP-ITGA4 shRNA cells transfected with Control siRNA (Con siRNA) or SUFU siRNA. Similar results were obtained in the repeated experiments. (E) Gene Expression Profiling Interactive Analysis (GEPIA) on the correlation between ITGA4 and GLI-1 expression in lung cancer patients. (F) Gene set enrichment analysis (GSEA) of the Hedgehog pathway gene sets associated with ITGA4 high expression. (G) Effect of treatment with a Hedgehog pathway agonist Purmorphamine (24 h) on the protein levels of SHH, SMO, GLI-1 and SUFU in BEAS-2B–As + BaP-ITGA4 shRNA cells. Similar results were obtained in the repeated experiments. (H) Effect of Purmorphamine treatment (5 μM) on the suspension culture sphere forming capability of BEAS-2B–As + BaP-ITGA4 shRNA cells (mean ± SD, n = 3). ** $p < 0.01$, compared to vehicle control-treated cells.

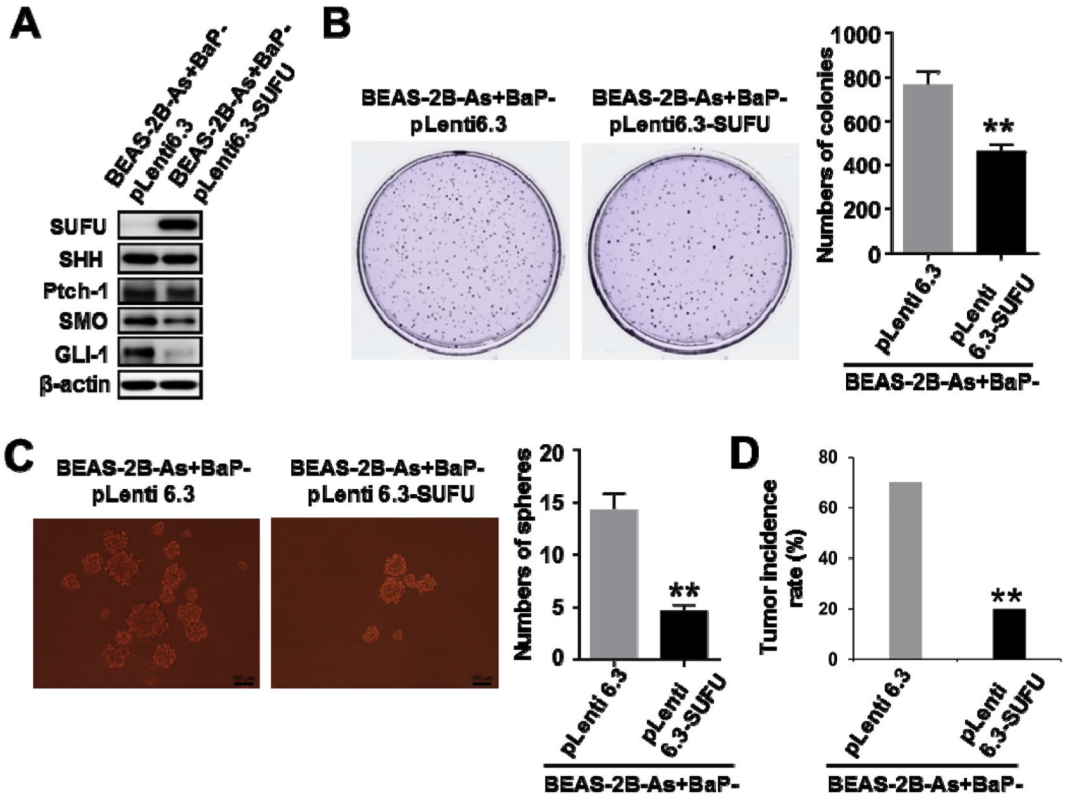

Fig. 4.

Stably overexpressing SUFU in arsenic and BaP co-exposure-transformed cells significantly reduces the Hedgehog pathway activation, CSC-like property and tumorigenicity. (A) Representative Western blot analysis of SHH, Ptch-1, SMO, SUFU and GLI-1 protein levels in vector control and SUFU stably overexpressing BEAS-2B–As + BaP cells. Similar results were observed in the repeated Western blots. (B–C) Effect of stably overexpressing SUFU in arsenic and BaP co-exposure-transformed cells on their capability of forming soft agar colonies (B) and suspension culture spheres (C) (mean ± SD, n = 3). ** $p < 0.01$, compared to BEAS-2B–As + BaP-pLenti6.3 vector control cells. Similar results were observed in the repeated experiments. (D) The tumor incidence rate in mice injected with BEAS-2B–As + BaP-pLenti6.3 vector control or BEAS-2B–As + BaP-pLenti6.3-SUFU overexpression cells as described in Methods. ** $p < 0.01$, compared to mice injected with BEAS-2B–As + BaP-pLenti6.3 vector control cells.

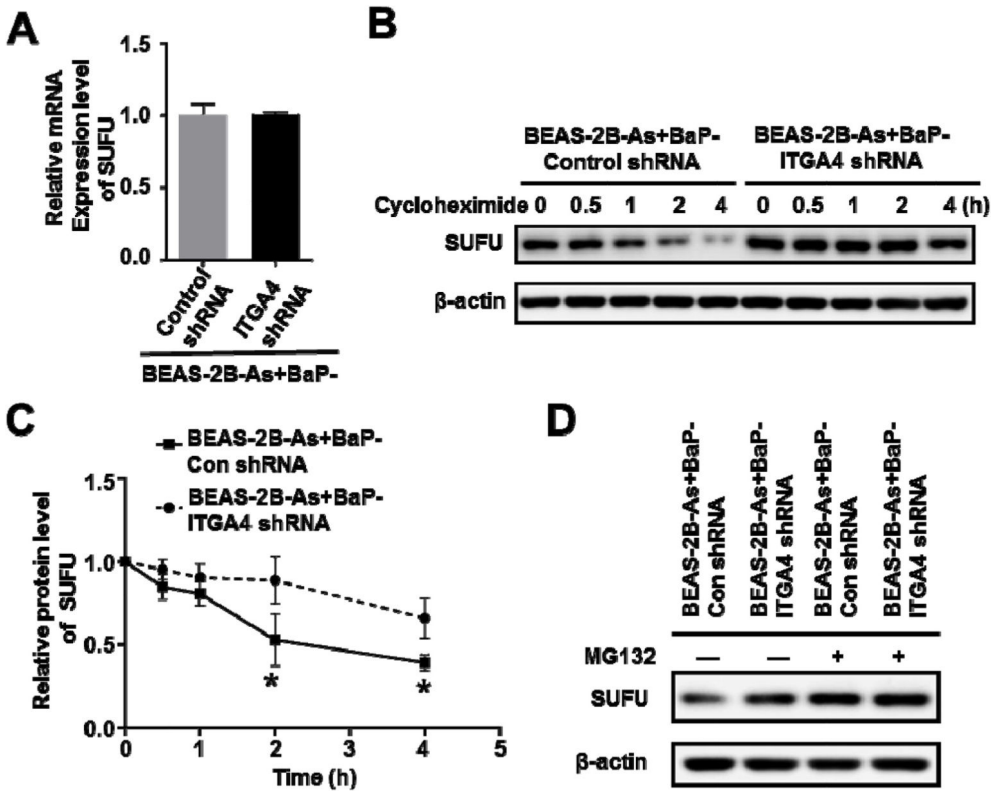

Fig. 5.

ITGA4 down-regulation in arsenic and BaP co-exposure-transformed cells up-regulates SUFU levels by increasing SUFU protein stability. (A) Q-PCR analysis of SUFU mRNA expression levels in shRNA vector control and ITGA4 stable knockdown BEAS-2B–As + BaP cells (mean ± SD, n = 3). (B–C) Representative Western blot analysis (B) and quantitated results (mean ± SD, n = 3) (C) of SUFU protein half-life in shRNA vector control and ITGA4 stable knockdown BEAS-2B–As + BaP cells treated with 5 μM of cycloheximide (CHX) for 0, 0.5, 1, 2, 4 h, respectively. * $p < 0.05$, compared to the BEAS-2B–As + BaP-Control shRNA cells. (D) Representative Western blot analysis of SUFU protein levels in shRNA vector control and ITGA4 stable knockdown BEAS-2B–As + BaP cells treated with a vehicle control or 10 μM of MG132 for 2 h. Similar results were obtained in the repeated experiments.

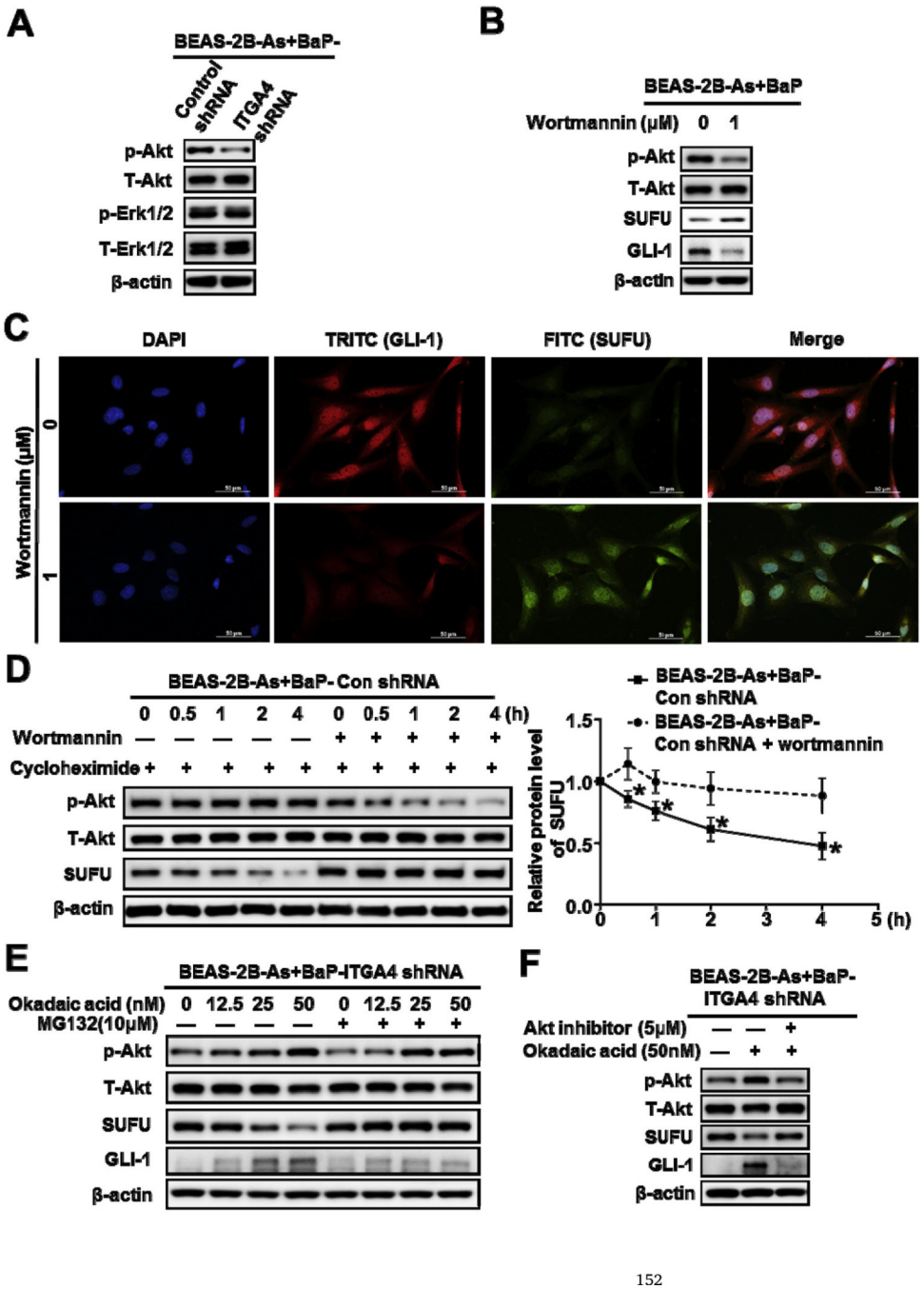

152

Fig. 6.

ITGA4 down-regulation in arsenic and BaP co-exposure-transformed cells reduces the PI3K/Akt Pathway Activity to increase SUFU protein stability. (A) Representative Western blot analysis of phosphor- and total Akt and Erk1/2 levels in shRNA vector control and ITGA4 stable knockdown BEAS-2B–As + BaP cells. (B) Representative western blot analysis of GLI-1 and SUFU protein expression levels in BEAS-2B–As + BaP cells treated with 1 μM of Wortmannin for 24 h. (C) Representative IF staining images and overlaid images of GLI-1 staining in red fluorescence, SUFU staining in green fluorescence and

nuclear DAPI staining in blue fluorescence. Scale bar: 50 μm. (D) Representative Western blot analysis and the quantitated results (mean ± SD, n = 3) of SUFU protein half-life in BEAS-2B–As + BaP cells treated with 5 μM of cycloheximide (CHX) for 0, 0.5, 1, 2, 4 h with a vehicle control or Wortmannin pretreatment (1 μM, 4 h). * $p < 0.05$, ** $p < 0.01$, compared to the BEAS-2B–As + BaP cells treated with a vehicle control. (E) Representative Western blot analysis of phosphor- and total Akt, GLI-1 and SUFU protein levels in ITGA4 stable knockdown BEAS-2B–As + BaP cells pre-treated with Okadaic acid (0, 12.5, 25, 50 nM) for 24 h plus a vehicle control or 10 μM of MG132 treatment for 2 h. (F) Representative Western blot analysis of phosphor- and total Akt, GLI-1 and SUFU protein levels in ITGA4 stable knockdown BEAS-2B–As + BaP cells treated with a vehicle control, Okadaic acid (50 nM) or AKT inhibitor (5 μM) plus Okadaic acid (50 nM) for 24 h. Similar results were obtained in the repeated experiments.

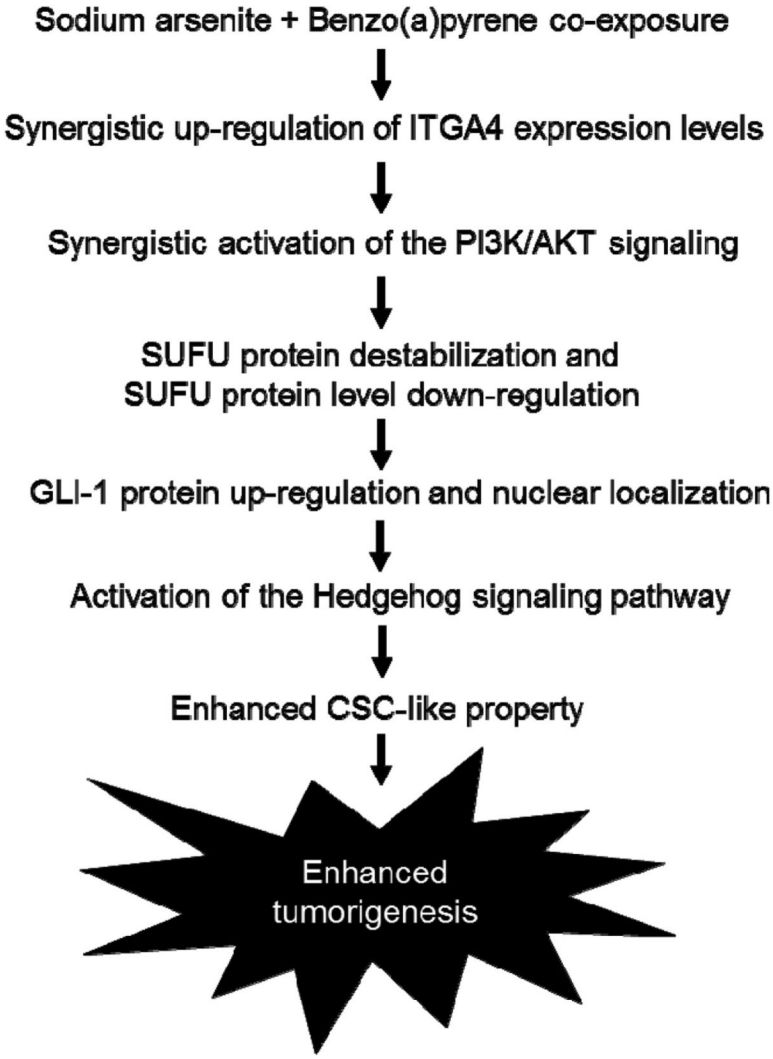

Fig. 7.

A schematic summary of how arsenic and BaP co-exposure increases cancer stem cell-like property and enhances tumorigenesis.